Completing the Development of the 12.5 kW Hall Effect Rocket with Magnetic Shielding (HERMeS)

IEPC-2019-193

Presented at the 36th International Electric Propulsion Conference
University of Vienna • Vienna, Austria
September 15-20, 2019

Richard Hofer*, Robert Lobbia†, Vernon Chaplin‡, Alejandro Lopez Ortega§, Ioannis Mikellides**, James Polk††
Jet Propulsion Laboratory, California Institute of Technology, Pasadena, CA, USA

Hani Kamhawi‡‡, Jason Frieman§§, Wensheng Huang***, Peter Peterson,††† Daniel Herman‡‡‡
NASA Glenn Research Center, Cleveland, OH, USA

The Hall Effect Rocket with Magnetic Shielding (HERMeS) is a 12.5 kW Hall thruster co-developed by NASA Glenn Research Center and the Jet Propulsion Laboratory. HERMeS incorporates magnetic shielding to eliminate discharge channel erosion in order to reach its design lifetime of 50 kh at specific impulses up to 3000 s. The capabilities of the HERMeS thruster technology transferred to Aerojet Rocketdyne under the Advanced Electric Propulsion System (AEPS) program are described. HERMeS hardware testing is now focused at reducing risk and supporting the qualification of the AEPS thruster. These includes a series of progressively longer wear tests, plasma characterization and modeling supporting life qualification, magnetic field optimization, and environmental testing. Initial results from AEPS thruster testing show operation consistent with the HERMeS thrusters and steady-state operation has been achieved at 600 V, 12.5 kW.

* SEP Thruster Lead, richard.r.hofer@jpl.nasa.gov
† SEP Thruster Environmental Test Lead
‡ SEP TDU-2 LIF Test Lead
§ SEP Plasma Modeling Engineer
** SEP Plasma Modeling Lead
†† SEP Thruster Life Qualification Lead
‡‡ SEP Test Lead
§§ SEP Thruster Wear Test Lead
*** SEP Plasma Diagnostics Lead
††† SEP Project Lead Engineer
‡‡‡ PPE Ion Propulsion System Lead

I. Introduction

NASA is charged with leading an exploration program with commercial and international partners that enables human expansion across the solar system [1]. The program is an evolutionary architecture extending beyond low-Earth orbit that aims to return humans to the Moon followed by missions to Mars and other destinations. High-power solar electric propulsion (SEP) is an enabling technology incorporated in this architecture because of its potential to advance these directives [2]. Specifically, 50 kW-class electric propulsion (EP) systems and flexible blanket solar arrays have been identified to provide significant capabilities that are readily scalable to much higher power systems [3-6].

NASA recently announced plans to send astronauts to the Lunar surface by 2024 as part of the newly formed Artemis program. A key aspect of the Artemis program is the Luna Gateway, which is envisioned as a maneuverable outpost in cis-lunar space that will extend human presence to deep space and provide access to the surface of the Moon. The first element of the Gateway is the Power and Propulsion Element (PPE), illustrated in Figure 1, in which NASA recently announced a commercial partnership to demonstrate a high-powered SEP spacecraft with Maxar Technologies (formerly SSL). The PPE exploration mission, illustrated in Figure 2, will reach and maintain lunar orbit by incorporating two high-powered SEP systems: one developed by NASA under contract with Aerojet Rocketdyne (AR) and the other a Maxar developed system augmented with NASA funding under a Tipping Point contract [2]. The PPE is baselined to include two 12.5 kW discharge power Hall thruster systems from AR's Advanced Electric Propulsion System (AEPS) [7,8] and a Maxar-developed system comprising four Busek 6 kW Hall thrusters and Maxar-developed power processing units (PPU) [2]. The combined 50-kW class solar electric propulsion (SEP) system will primarily be used for orbit transfers and station keeping, but can also provide attitude control and momentum management.

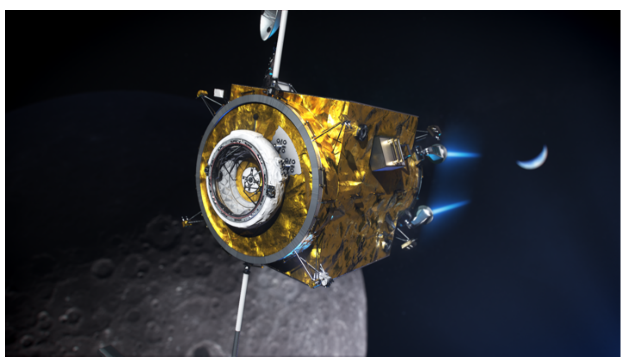

Figure 1. NASA concept illustration of the Power and Propulsion Element (PPE), the first element of the Lunar Gateway. [Credit: NASA]

Since 2012, NASA has been developing a high-power Hall thruster EP string that can serve as a building block for realizing a 50 kW-class propulsion system capability [7,8]. The Hall thruster system development, led by the NASA Glenn Research Center (GRC) and the Jet Propulsion Laboratory (JPL), began with in-house maturation of a 12.5 kW Hall thruster and associated PPU. The technology development work has since transitioned to AR via a competitive procurement for the AEPS contract that started in May 2016 [9]. The AEPS EP string consists of the Hall thruster, PPU, xenon flow controller (XFC), and harnesses. Figure 3 shows the AEPS Engineering Test Unit-1 (ETU-1), which started hot fire testing at JPL in August 2019 [10].

NASA continues to support the AEPS development leveraging in-house expertise, plasma modeling capability, and test facilities. This paper provides an overview of the tasks that NASA has executed since our last report in Ref. [11]. Several related papers provide additional detail on these and other topics [12-48]. In the next section, the capabilities of the HERMeS technology that was transferred to AEPS are summarized. This is followed by a discussion of recent NASA activities aimed at reducing risk and supporting the qualification of the AEPS thruster.

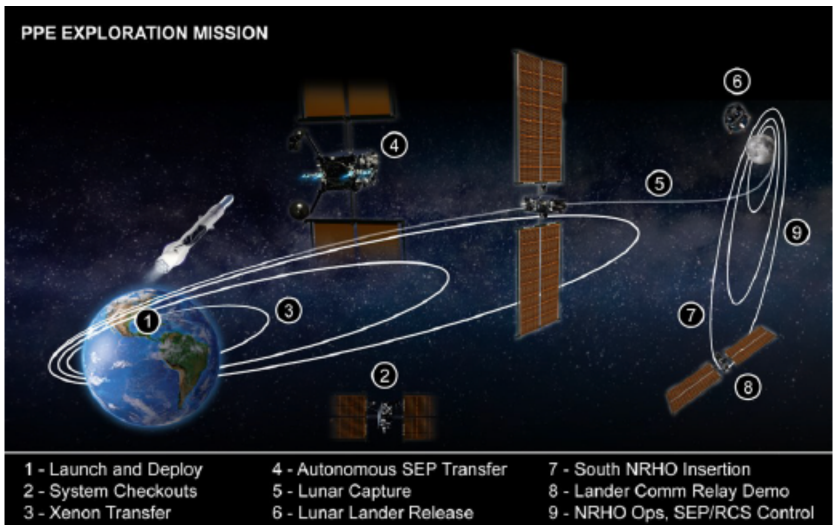

Figure 2. Notional concept of the PPE Exploration Mission described in Ref. [2].

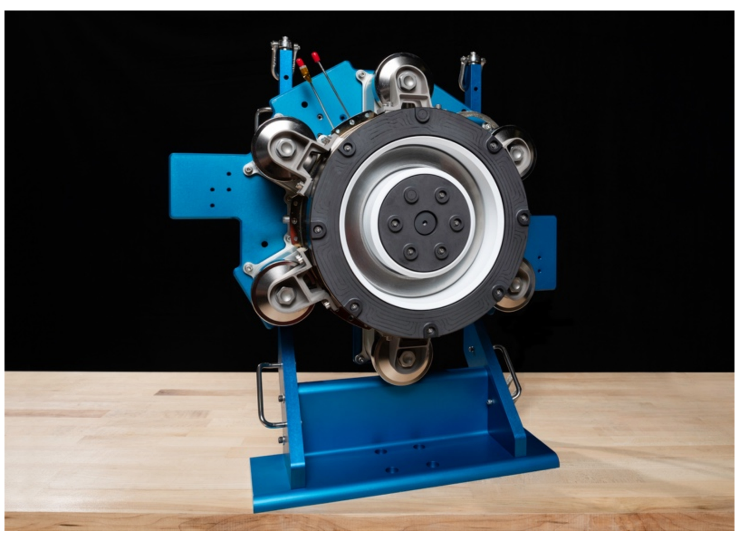

Figure 3. The AEPS Engineering Test Unit 1 (ETU-1) Hall Thruster prior to first operation in August 2019.

II. Thruster Capabilities

Shown in Figure 4, the Hall Effect Rocket with Magnetic Shielding (HERMeS) is designed to operate at 12.5 kW discharge power and up to 3000 s specific impulse with a service life of 50 kh [49,50]. At the 600 V maximum operating voltage required for the AEPS flight system, HERMeS produces in excess of 2800 s specific impulse and a thrust efficiency (exclusive of the PPU) of 67%. A design life of 50 kh is achieved through the use of magnetic shielding that eliminates discharge chamber erosion as a wearout failure mode. Against the design life, the AEPS flight system will require a seemingly modest 23 kh of operation (equivalent to 1700 kg of xenon throughput), but this still represents more than a factor of two greater operating time than previous Hall thruster flight systems such as the AR XR-5 or the Fakel SPT-140.

Hall thrusters are now capable of meeting such extraordinary lifetime requirements due to the breakthrough advances enabled by magnetic shielding [51-55], a technology that decreases discharge chamber erosion by orders of magnitude. Magnetic shielding physics were first identified through numerical simulations performed by JPL of AR's XR-5 Hall thruster [51,52], subsequently validated through simulations and experiments on the magnetically shielded H6MS Hall thruster [54-56], and then extended to high-specific impulse [57,58] high-power [59,60] and low-power thrusters [61,62].

HERMeS is the first Hall thruster designed with magnetic shielding over its entire service life and brings together advances in thruster performance and lifetime from NASA research since the turn of the century [49]. To achieve its design goals, HERMeS uses an integrated magnetic and thermal design, graphite pole piece covers, a cathode-tied electrical configuration [63], an internally mounted cathode with a graphite keeper, and a downstream-plenum gas distributor [37].

Figure 4 The 12.5 kW HERMeS Technology Development Unit 3 (TDU-3).

Figure 5 depicts an operating envelope of HERMeS spanning 6.25-12.25 kW that has been refined during development testing [11,24,45] for use in a 40-kW Ion Propulsion System for missions extending as far as 2.45 AU [49].[§§§] While this operating envelope spans 300-800 V and

[§§§] The low-power portion of the operating envelope, as might be needed by a single thruster for deep-space destinations beyond Mars, is actually much lower than shown. For example, HERMeS has been demonstrated in the laboratory to operate as low as 300 V, 2 A.

11-31 A, the primary throttle curve of HERMeS spans 300-600 V at a constant discharge current of 20.8 A. Several Reference Firing Conditions (RFCs) are used to benchmark performance between different thruster builds and facilities. A low-power branch extending from 9 to 20.8 A is also shown at 300 V. This branch is used after system startup at 300 V, ~9 A until 20.8 A is reached and then the voltage is throttled to as high as 600 V.

Figure 6 shows the approximate thrust and specific impulse over the throttle curve and HERMeS operating envelope shown in Figure 5 as a function of thruster discharge power. Table 1 lists the average performance of HERMeS demonstrated over 3,600 h of operation during the Long Duration Wear Test of TDU-3 [45]. Thrust was essentially invariant with time because the discharge chamber does not erode. This is a key feature of magnetically shielded thrusters that significantly reduces the margins that mission planners must account for with thrusters with discharge chamber erosion and, as a result, experience time-dependent performance [64]. Over 6.3-12.5 kW discharge power, thrust varied from 396-613 mN, specific impulse from 1960-2830 s, and efficiency from 59.6-67.2%. Specific impulse includes the cathode flow rate and efficiency the cathode flow rate and magnet power.

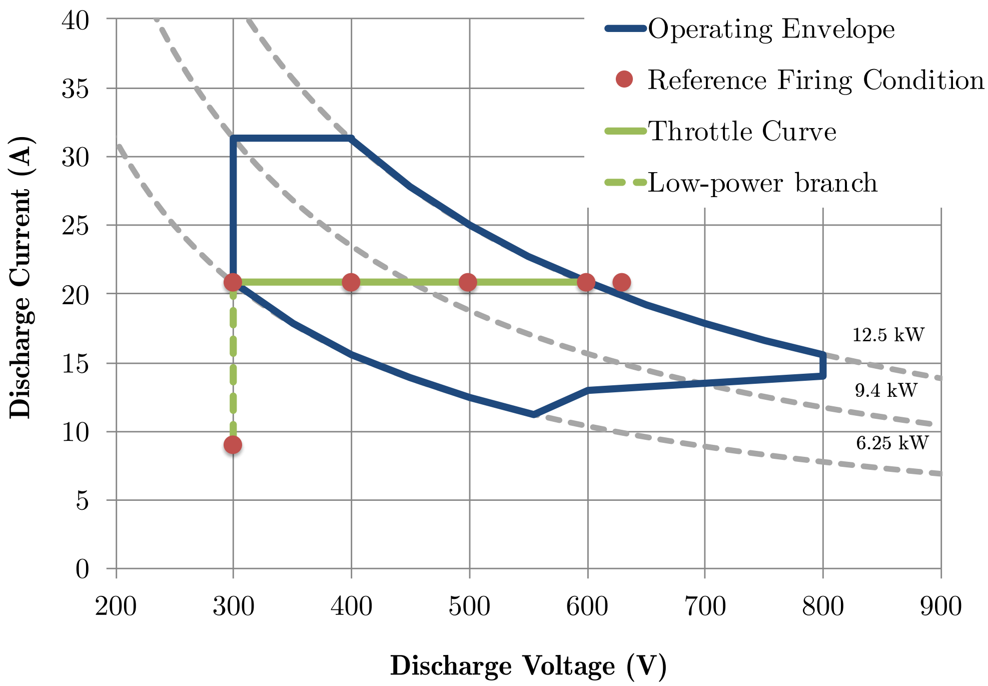

Figure 5 The HERMeS operating envelope for 6.25-12.5 kW discharge powers spans 300-800 V and 11-31 A. Also shown are the Reference Firing Conditions used during development testing, the primary throttle curve now used with AEPS, and a low-power branch at 300 V that is used at system startup.

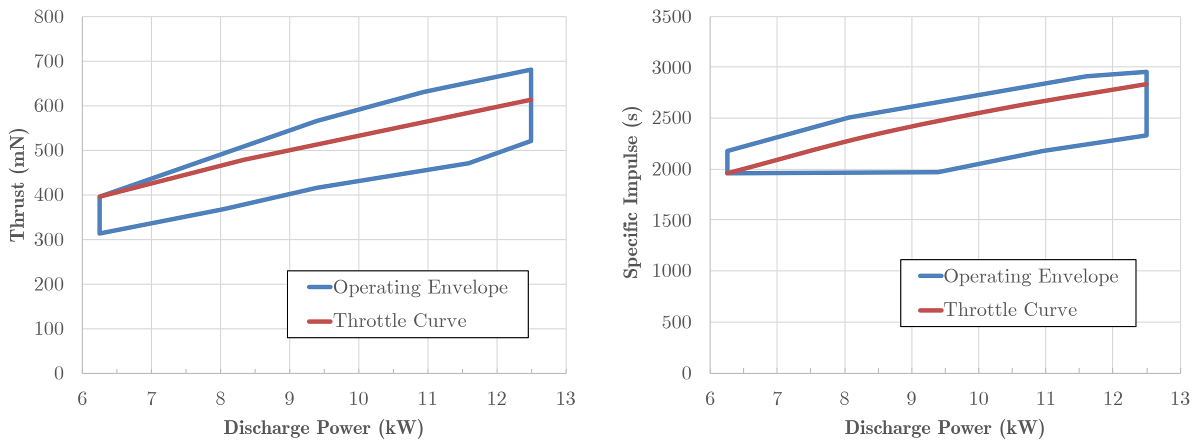

Figure 6 Approximate thrust and specific impulse capability of a HERMeS thruster versus thruster discharge power for the operating envelope shown in Figure 5.

Table 1 Average performance of HERMeS demonstrated over 3,600 h of operation during the Long Duration Wear Test of TDU-3 [45]. Thrust was essentially invariant with time because the discharge chamber does not erode.

RFC		Thrust (mN)		Specific Impulse (s)		Efficiency (%)	
		Mean	Standard Deviation	Mean	Standard Deviation	Mean	Standard Deviation
1	300 V, 2.7 kW	167.5	2.4	1760	26.5	51.1	1.5
2	300 V, 6.3 kW	395.5	2.2	1960	11.2	59.6	0.6
3	400 V, 8.3 kW	479.1	2.1	2321	12.9	64.4	0.6
4	500 V, 10.4 kW	545.7	2.4	2595	13.3	65.8	0.5
5	600 V, 12.5 kW	612.9	2.0	2826	11.8	67.2	0.4
6	630 V, 13.1 kW	630.3	2.2	2897	13.5	67.5	0.4

III. Risk Reduction and Life Qualification Activities

Wear testing, environmental testing, and physics-based plasma modeling validated through non-intrusive plasma measurements were the principal methods used to mature the HERMeS technology before being transferred to Aerojet Rocketdyne at the start of the AEPS program. Since then, and in addition to providing insight/oversight of the AEPS thruster development, thruster test and modeling activities at GRC and JPL have focused on risk reduction supporting the AEPS design, preparation for AEPS testing, and life qualification activities supporting AEPS. This section describes major elements of those activities.

A. Wear testing supporting life qualification

Magnetic shielding essentially eliminates discharge chamber erosion as the primary wearout failure mode in Hall thrusters. This greatly extends the service life of Hall thrusters, but other components are subject to wearout failure modes that must also be accounted for. Among these include pole erosion [36,65-68], several cathode failure modes (insert depletion or evaporation, keeper erosion, cathode orifice erosion, heater failure), electromagnet insulation failures, and other failure modes related to high-temperature operation and thermal cycling (e.g., propellant isolator or anode structural failures). An extensive discussion of our approach to qualifying the service life of the AEPS thruster is detailed in [35].

In order to assess these wearout failure modes and also to prepare for the planned 23 kh life qualification test of the AEPS EDU thruster, wear tests with durations ranging as short as 10 h [69] to as long as 3.6 kh [45] have been conducted with the H6MS [57,67] and HERMeS [34,66,70]. The approach is similar to the one taken with the development of the NSTAR ion thruster, which also included a series of progressively longer wear tests as confidence grew in the thruster design and testing methods [71,72]. HERMeS wear testing has focused on quantifying known and potentially unknown erosion modes of the discharge chamber, pole covers, and cathode. Plasma simulations are used concurrently to predict and interpret wear tests outcomes. Facility effects encountered during wear testing have also been a focus of these investigations. In particular, the effects of carbon deposition in the discharge chamber on thruster performance and stability are being closely studied. Finally, the wear tests are building the expertise with the thruster, diagnostics, and vacuum facility prior to starting the planned Figure 5 23 kh life qualification test. In the remainder of this section, we summarize the objectives and major results from these wear tests since our last report, which included summaries of prior efforts [11].

1. *H6MS Accelerated Carbon Deposition Campaign*

In order to assess the impact of backsputtered carbon on the AEPS thruster throughout the planned 23 kh qualification wear test and identify potential failure mechanisms related to ground testing, the Accelerated Carbon Deposition Campaign (AC/DC) was performed at JPL using the H6MS, a similar magnetically shielded 6-kW Hall thruster. Based on measured backsputter rates in VF-5 at GRC [73], where the wear test of the AEPS qualification thruster will occur, approximately 40-µm of carbon is expected to coat all downstream facing surfaces over 23 kh of operation. In order to simulate these conditions in the AC/DC, the carbon backsputter rate was accelerated by 54 times by placing a 1-m×1-m graphite plate 0.5 m downstream from the thruster and then operating the thruster until 40-µm of carbon deposition was recorded, which required 0.4 kh of thruster operation at 300 V, 6 kW (see Figure 7).

Across the 0.4 kh of the AC/DC, thrust and specific impulse remained invariant as did many other operational parameters including thruster steady-state temperatures. The amplitude of discharge current oscillations increased 46% while the overall features of the oscillation spectra (peak locations and widths) remained unchanged. The boron nitride discharge channel walls became effectively conductive with 36 Ω average surface resistance after the test. The anode to body/cathode high-voltage isolation resistance dropped from GΩ values to 50 kΩ with no measurable loss in performance. Numerous carbon flare and spark events were observed that led to unexpected thruster shutdowns approximately every six hours, which would correspond to a shutdown every 14 days in a non-accelerated test. After the first dozen unexpected shutdowns, the cathode keeper was operated continuously to keep the thruster lit throughout these spark events. Evaluation of the time-resolved discharge signals showed that these spark events sometimes reached current levels of 400 A. Large scale spalling events were also observed while the thruster underwent large thermal transients (e.g. after shutdown), suggesting that the mismatch in the coefficients of thermal expansion for the carbon and iron pole pieces are the main carbon spalling mechanism.

The success of the AC/DC reduces the risk of performing the planned 23 kh AEPS qualification thruster wear test by demonstrating negligible performance/stability effects, robustness against shorting events and carbon spalling, and dramatic decreases in insulation resistance. The results of the AC/DC are consistent with previous wear tests of the H6MS and HERMeS TDU thrusters that have been conducted up to 3.6 kh of operation [34,45,57,66,67,70].

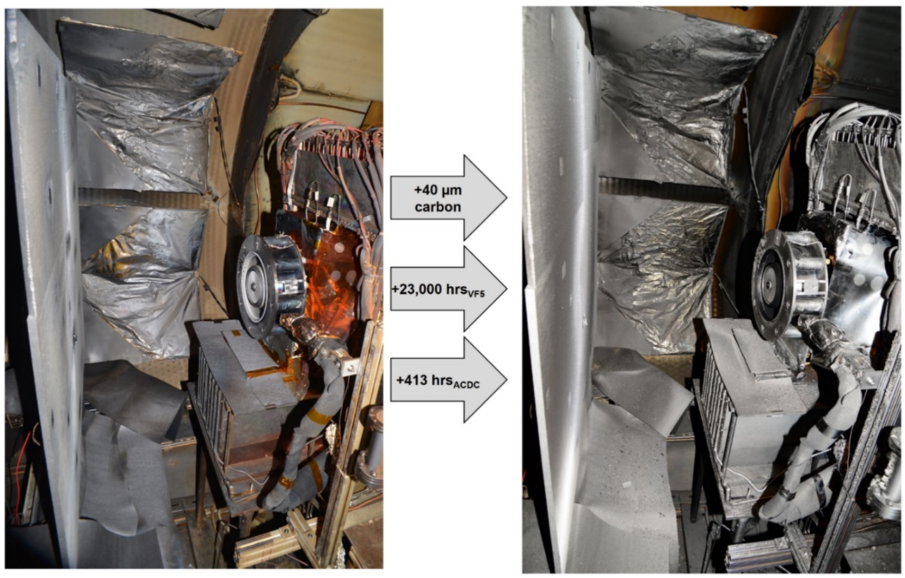

Figure 7. Photographs of the test configuration before (left) and after (right) used in the Accelerated Carbon Deposition Campaign (AC/DC) at JPL [44]. Shown are the H6MS Hall thruster mounted on a thrust stand and the graphite target used to accelerate the carbon backsputter rate. After 0.4 kh of operation in this configuration, 40 μm-carbon were deposited on the thruster, corresponding to 23 kh of equivalent runtime in the GRC VF-5 vacuum chamber that will be used for wear testing of the AEPS qualification thruster.

2. TDU-3 long duration wear test

Extensive wear testing with HERMeS has been conducted to validate the design, identify wear mechanisms, and provide data used in the development of physics-based service life models of the thruster. Erosion of the graphite pole covers has supplanted discharge chamber erosion as the primary wearout failure mode. Understanding the physics of pole cover erosion and the worse-case operating conditions at which it occurs has led to a series of wear tests that were summarized previously in Ref. [11]. Pathfinding wear tests with the H6MS [57,67] led to the TDU-1 wear test in 2016 that accumulated 1,700 h of operation [66,74]. This was followed in 2017 with the TDU-3 thruster in the Short Duration Wear Test (SDWT), which consisted of seven, approximately 200 h segments that varied the thruster configuration or operating conditions [70]. Finally, over October 2017 to October 2018 the Long Duration Wear Test (LDWT) of TDU-3 was conducted to quantify performance, stability, plume, and wear trends and prepare for the qualification wear test of the AEPS thruster [34,45]. Figure 8 shows TDU-3 installed for the LDWT, which concluded after 3,600 h of operation. Including the time from the SDWT, the discharge chamber and anode assembly have been subjected to 4,500 h of operation while the emitter in the hollow cathode, after adding time from its use in the TDU-1 wear test, has been operated for 6,200 h. Performance, stability, and plume properties during the LDWT were invariant while measured erosion rates were consistent with the design lifetime. Table 1 lists the average performance of TDU-3 from the LDWT. Figure 9 shows the thrust (left, middle) as a function of time and the erosion rates (right) measured on the inner front pole cover. The results were consistent with earlier performance and wear testing of magnetically shielded Hall thrusters [34,45,57,66,67,70] where erosion of the discharge chamber was not detected and thruster performance was essentially constant with time. The measured erosion rates on the inner front pole of TDU-3 were found to be consistent with meeting the 23 kh life requirement with at least 50% margin (i.e., >35 kh). The conclusion of the LDWT has established that the life of the HERMeS design will meet the AEPS thruster requirements and that the diagnostics and vacuum facility are ready to support the qualification wear test.

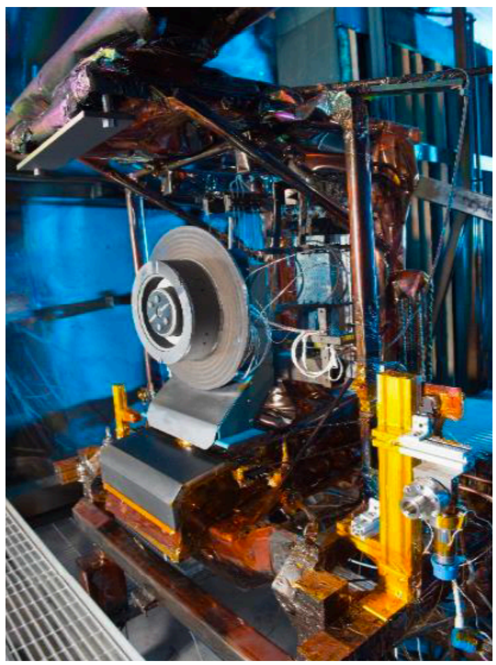

Figure 8. HERMeS TDU-3 installed for the Long Duration Wear Test in Vacuum Facility 5 at NASA GRC. Wear testing of HERMeS is used to establish the service life of the thruster predicted by physics-based modeling [45].

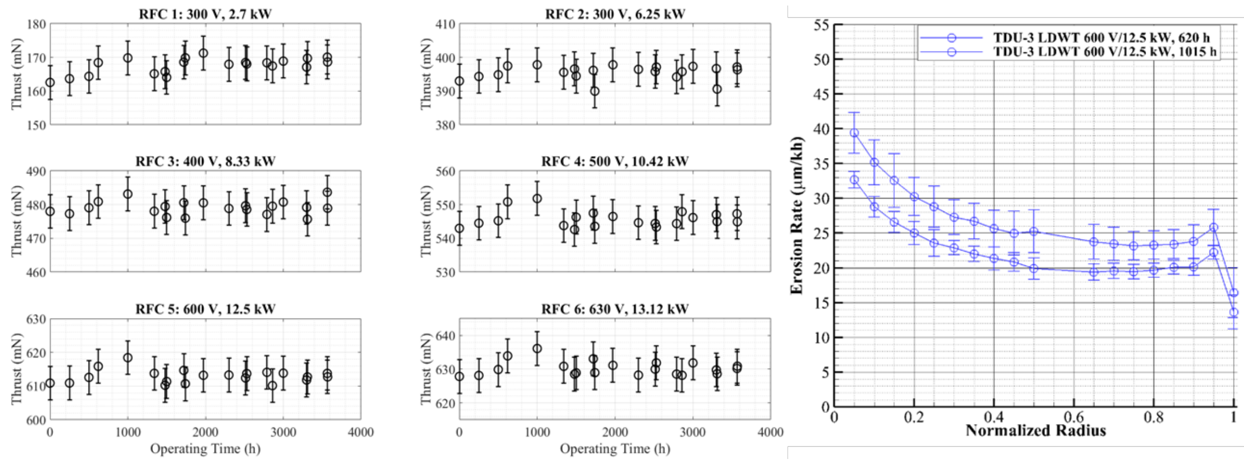

Figure 9. TDU-3 thrust (left, middle) as a function of operating time during the TDU-3 LDWT and inner front pole cover erosion rates (right) measured during the first segment of the test [45].

3. H9C Extremely Late-in-Life test

The Accelerated Carbon Deposition Campaign (AC/DC) at JPL [44], which simulated 23 kh of carbon deposition over 0.4 kh of testing, and the TDU-3 Long Duration Wear Test (LDWT) at GRC, which accumulated a total of 3.6 kh of thruster operation [45], both observed marked decreases in the anode to cathode (body) impedance, ostensibly due to the accumulation of backsputtered carbon on the channel walls and carbon flakes bridging the gap between the channel walls and the thruster body. Thruster operation continued to be nominal in the AC/DC and the LDWT despite the reduction of anode-cathode isolation, but these observations are still viewed as a risk to the successful completion of the wear test of the AEPS qualification thruster. In order to address this risk, the Extremely Late-of-Life (ELL) test was conducted at JPL that ran the H9 Hall thruster [75], operating at 600 V and the equivalent current and power density as AEPS, with a discharge chamber fabricated from graphite and electrically tied to the anode (Figure 10). This thruster configuration, referred to as H9C, was selected to simulate late-in-life conditions of the ceramic walls of the AEPS thruster, which will be covered in electrically conducting carbon backsputtered from the thruster and the vacuum facility during the qualification wear test.

The H9C is a unique test configuration that, unlike that experienced in a wear test, allows for precise control of the wall electrical characteristics. The thruster was operated with the body tied to cathode and with the walls either electrically floating or tied to the anode over 300-600 V and up to 9 kW. There were no issues igniting the plasma and thruster operation appeared to be indistinguishable from operation with ceramic walls. Initial tests results, which are summarized in Table 2, show that that anode flow rate was about 2% lower with the H9C compared to operation with boron nitride (BN) walls, which possibly indicated that the approximately 6 A of current flowing through the walls partially leaked to the anode. This could result in a decrease in performance, but this brief test did not allow for thrust measurements. The amplitude of discharge current oscillations was unchanged. The amount of current flowing through each wall could be controlled by adjusting the shape of the magnetic field topology through adjustments of the thruster coil currents. Similar to earlier tests at JPL of conducting wall thrusters with magnetic shielding conducted at 300 V [76], if floated, the walls would reach to within a few volts of the anode potential.

The ELL test of a 600 V, 9 kW thruster operating with a graphite wall represents an extreme version of the AC/DC and LDWT, and demonstrates that magnetically-shielded Hall thrusters are remarkably robust against ground test facility effects related to backsputtered carbon, thereby reducing the risk to the wear test of the AEPS qualification thruster. Closure of this risk requires further testing that includes thrust measurements and testing that attempts to simulate electrical shorts between the anode to cathode and other events related to materials spalling from thruster surfaces.

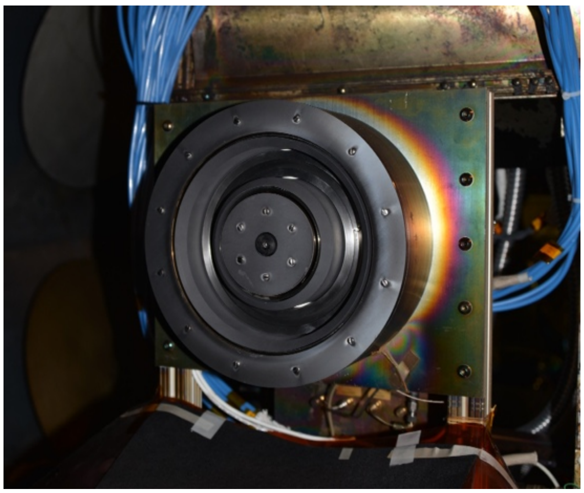

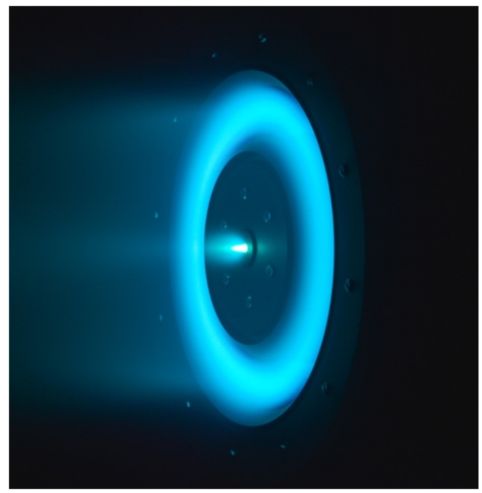

Figure 10. The H9C installed (left) at JPL for the Extremely Late-of-Life test and operating (right) at 600 V, 9 kW. Graphite was used for the discharge chamber walls to simulate the highly-conductive state of the walls after long duration wear testing.

Table 2. Comparison of the H9 with boron nitride (BN) versus graphite (C) walls over 300-600 V and a maximum power of 9 kW. The amplitude of discharge current oscillations was unchanged. The anode flow rate was about 2% lower with the H9C, which possibly indicated that the approximately 6 A of current flowing through the walls partially leaked to the anode.

		H9 - BN	H9 - C	H9 - BN	H9 - C		
Disharge Voltage (V)	Discharge Current (A)	Discharge RMS (A)	Discharge RMS (A)	Anode flow rate (mg/s)	Anode flow rate (mg/s)	Anode flow % difference	H9C - Wall Current (A)
300	20	0.99	0.96	17.9	17.5	-2.2%	6.7
400	15	1.34	1.10	14.9	14.5	-2.7%	5.5
500	15	1.84	1.79	15.3	15.0	-2.1%	5.8
600	15	2.30	1.79	15.5	15.1	-2.3%	5.9

B. Plasma modeling and non-invasive diagnostics supporting life qualification

As depicted in Figure 11, physics-based plasma modeling empirically-informed and validated through non-intrusive plasma measurements and wear testing are being integrally used as part of the service life qualification for the AEPS thruster [14,36,38,42]. JPL's Hall2De [77-79] and OrCa2D [80-83] plasma models provide simulations of the thruster and cathode, respectively. Typical results from Hall2De and OrCa2D are shown in Figure 12 for the plasma density in the Hall thruster (top) and hollow cathode (bottom). Analytical and numerical models of the vacuum chamber environment and the transport of carbon sputtered from the facility and the thruster have also been developed at GRC [15,73,84,85]. A more detailed discussion of the plasma modeling and validation experiments was provided in our previous report [11].

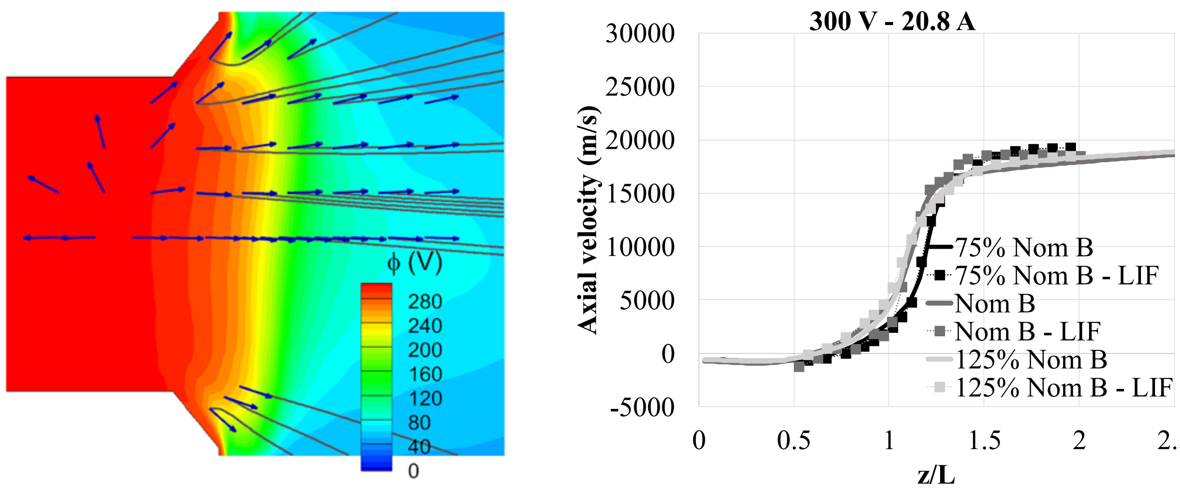

Figure 11 Physics-based plasma modeling validated through non-intrusive plasma measurements are integrally used as part of the service life qualification for the AEPS thruster [14,36,38,42]. Left: 2-D comparison between singly charged ion streamlines from JPL's Hall2De and unit vectors of the ion velocity field from LIF measurements at nominal magnetic field strength. The velocity fields are overlaid on the computed contours of the plasma potential. Right: Comparison of the LIF and computed axial ion velocities along the channel centerline at different strengths of the magnetic field.

OrCa2D was employed to perform numerical analyses of the HERMeS cathode, with the objectives to assess depletion/vaporization of the emitter material and erosion of the cathode plate and keeper electrodes. The OrCa2D simulations were supported by Hall2De to determine the contribution of ions from the thruster to the erosion of the keeper. The results of the cathode simulations with OrCa2D are reported in Ref. [86] and summarized in Ref. [11].

Hall2D has been used to investigate the full throttling envelope of HERMeS, consisting mostly of operation at the nominal discharge current of 20.8 A, a discharge voltage range of 300-600 V, and across a range of magnetic field intensities spanning 75-125% of nominal. Simulation results are validated through comparisons with a wide range of thruster measurements. The first measurements of the time-averaged ion velocity distribution function (IVDF) using laser-induced fluorescence (LIF) on HERMeS were completed on TDU-2 at JPL [87]. These measurements allowed comparisons with simulation results away from the channel centerline, and led to improvements in our understanding of both the anomalous collision frequency and the erosion of the thruster's pole covers. Time-averaged LIF diagnostics are also now in place at GRC that will be used to collect data on the AEPS ETU-2 thruster after it is delivered this year [22,23,41,42].

Results from the JPL and GRC LIF diagnostics, conducted on two different TDU thrusters in two different vacuum facilities, have shown excellent agreement (see Figure 13).

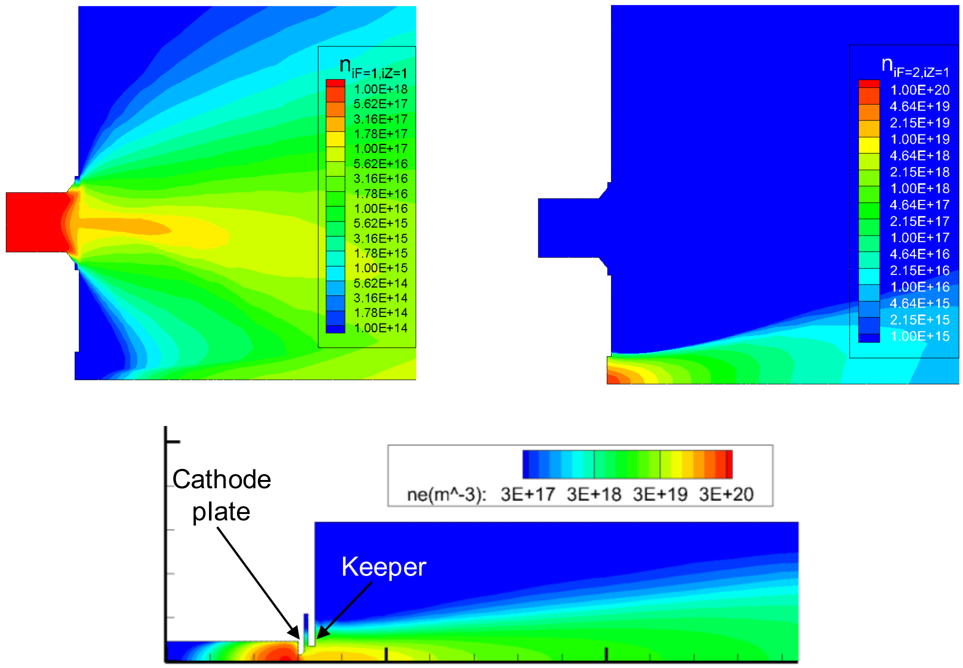

Figure 12 Top: JPL Hall2De simulation results of the ion number density (m^{-3}) of singly-charged ions in HERMeS at a discharge current of 20.8 A and nominal magnetic field. Left-top: ions generated in the acceleration channel (Fluid #1). Right-top: ions generated in the cathode plume (Fluid #2). Bottom: JPL OrCa2D simulation result for the electron number density in the HERMeS cathode operating with a BaO emitter at 20.8 A and nominal applied magnetic field.

Plasma simulations of the inner front pole cover (IFPC) wear currently underpredict the erosion rates at 300 V, 20.8 A for which wear tests have shown the highest values. The physics that drive the erosion at this operating condition appear to be unusual since the Hall2De simulations have successfully reproduced the measured wear rates at 600 V, 20.8 A [88]. Hall2De has also been used successfully to model pole cover erosion in the H6US and H6MS at 300 V (20 A) [36], as well as in the Magnetically-Shielded Miniature (MaSMi) thruster at operating conditions between 200 and 500 V [89]. Thus, the current focus of the modeling effort is to identify the source(s) of the discrepancy between simulation and measurement in HERMeS at 300 V [30]. To this end, recent LIF measurements by Huang, et al. [42] and Chaplin, et al [38] near the IFPC have shown ions from the cathode plume region diverging radially away from the thruster centerline, and that some of these ions impact the IFPC at mean energies that exceed the sputtering threshold. These measurements prompted a renewed interest in the question of whether the contribution to the IFPC erosion by high-energy ions from the cathode is significant, as first posed by Polk, et al. who performed electrostatic energy analyzer measurements of a HERMeS cathode operating with a magnetic simulator [69]. Thus, Hall2De simulations were performed soon thereafter and improved more recently to capture very well the ion velocity field measured by

Huang, et al. [42] and Chaplin, et al [38]. The new simulations show that the flux of cathode ions at the measured mean energies is not sufficient to explain the wear at 300 V. This finding is consistent with the abovementioned modeling results for HERMeS (at 600 V), H6MS and MaSMi which showed that the contribution of cathode ions was not significant. It is also worth noting that recent MS optimization tests with HERMeS operating at 600 V by Kamhawi, et al. [48], a summary of which follows in Section III.C below, showed a reduction of the IFPC wear, by about a factor of ~3, as the magnetic field topology was retracted towards the anode while keeping the cathode location and flow fraction unchanged. These observations were consistent with those in the H6 where it was found that, with the same cathode, the pole wear rates were significantly lower in the unshielded H6US compared to the magnetically shielded H6MS. From experimental investigations of the H6MS, Jorns, et al. [65] also argued that to fully explain the measured pole erosion, a population of ions with energies greater than 100 V must have been present but were at too of a low density to resolve with plasma diagnostics. Simulations by Lopez Ortega, et al. [36] showed that this population of ions indeed existed but it was not associated with the cathode ions. The HERMeS team is currently considering mechanisms by which the cathode plume may be coupling differently with the thruster ions under certain operating conditions and/or magnetic field topologies, possibly leading to IVDFs with wide spreads near the IFPC.

Figure 14 depicts time-resolved LIF (TR-LIF) measurements of the IVDF in HERMeS TDU-2 at JPL showing that the acceleration region oscillates in time at 600 V [38]. Incorporating these oscillations in Hall2De increased the inner pole erosion rate by a factor of 5-10, bringing the simulations at this discharge voltage into agreement with wear test results [88]. Unlike other TR-LIF techniques, the transfer function averaging technique [90,91] used at JPL did not rely on external perturbations or an assumption of periodicity and therefore was applicable to studying ion dynamics in HERMeS in both the periodic (discharge voltage = 500-600 V) and aperiodic (discharge voltage = 300-400 V) discharge oscillation regimes. The bandwidth of the transfer function averaged TR-LIF diagnostic was extended to ~100 kHz to resolve HERMeS discharge oscillations with fundamental frequency of ~55 kHz, a factor of greater than five higher than had been demonstrated previously with this technique.

TR-LIF measurements were carried out both along the channel centerline and in the beam edges, allowing detailed validation of the time dependent anomalous transport profile in the plasma models. The oscillations in the acceleration region location at 500-600 V were found to be impulsive rather than sinusoidal, with a rapid transition between the upstream and downstream positions. Larger-than-anticipated ion velocity oscillations in the near plume implied that the plasma potential in this region was varying by more than 100 V over the discharge oscillation period. Non-negligible temporal variations were detected in the IVDFs at 300-400 V, despite the small amplitude of the irregular discharge current oscillations at these conditions, but there did not appear to be sufficient dynamics in the inner beam edge to resolve the discrepancy between the measured and simulated inner pole cover erosion rates at 300 V.

Collectively, the combined efforts of JPL and GRC to conduct non-invasive LIF measurements of the thruster plasma are reducing risk by providing the empirical inputs necessary to determine the anomalous cross-field transport profile, improving our understanding of the ion dynamics, and providing the validation data necessary for Hall2De simulations used for life qualification.

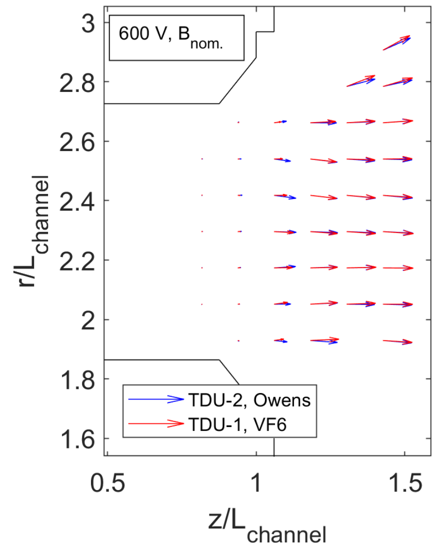

Figure 13. Comparison of ion velocity vectors measured with LIF on two different TDU thrusters in two different vacuum facilities at 600 V, 20.83 A and the nominal magnetic field intensity [38].

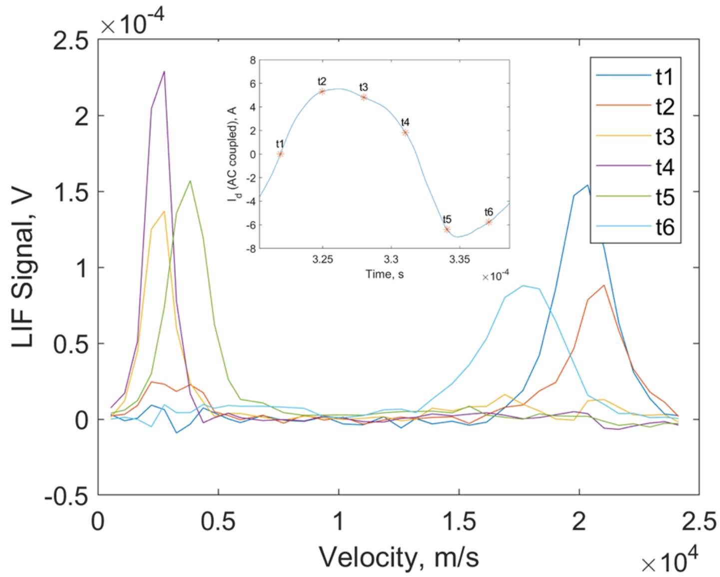

Figure 14. Time-resolved measurements of the IVDF in HERMeS TDU-2 at JPL show that the acceleration region oscillates in time at 600 V, 20.83 A providing critical validation data for plasma simulations using Hall2De [38].

C. Magnetic Field Optimization

During the design phase of the HERMeS thruster, the approach was to design a magnetic circuit that leveraged all the lessons learned from the H6MS and the NASA-300MS thruster work [54,59]. The TDU magnetic field topology was shielded to assure that discharge channel erosion was eliminated. This was validated by the wall probe test that was performed at discharge voltages up to 800 V [92]. The wear tests of the HERMeS TDU-1 and TDU-3 thruster found that discharge erosion rates were minimized; however, measurable erosion of the front pole covers, although lower than discharge channel erosion rates of unshielded thrusters, was found rendering it as the next life-limiting mechanism [18,45,48,66,69]. The objectives of the magnetic field optimization tests are to evaluate several candidate magnetic field topologies in an effort to find a balance between discharge channel erosion and front pole erosion while maintain the performance and stability of the HERMeS thruster and meeting the lifetime requirements for high-power NASA SEP mission concepts.

Magnetic field optimization tests were performed on the TDU-1 Hall thruster. Besides the baseline configuration (B0), three candidate magnetic field topologies (B1, B2 and B4) were designed, modeled, and tested. Testing of the candidate magnetic field topologies was performed at the NASA GRC VF-6 vacuum facility in two phases. During Phase I, LIF measurements were performed on the baseline (B0) and candidate magnetic field topologies (B1, B2, and B4). In Phase II, the performance, stability, wear (except for B4), plasma plume, and optical emission spectroscopy measurements were performed to provide data to assess the optimal configuration. Figure 15 (left) shows the thrust efficiency during thruster operation at 600 V, 12.5 kW and different magnetic field configurations. The results indicate that within the uncertainty of the measurement, the performance of the B0 and B2 configurations is almost identical across the various magnetic field settings of the thruster. Figure 15 (right) presents the normalized discharge current RMS magnitudes during the thruster's magnetic mapping test and different magnetic field configurations. The results show that, in general, the B2 configuration attained lower discharge current oscillation levels than B0, B1, and B4 configurations. The wear test results found that inner front pole cover erosion rates of configurations B1 and B2 were on average 65% and 39% lower than the configuration B0 rates. Additional details of the Magnetic Field Optimization can be found in Ref. [25,26,48].

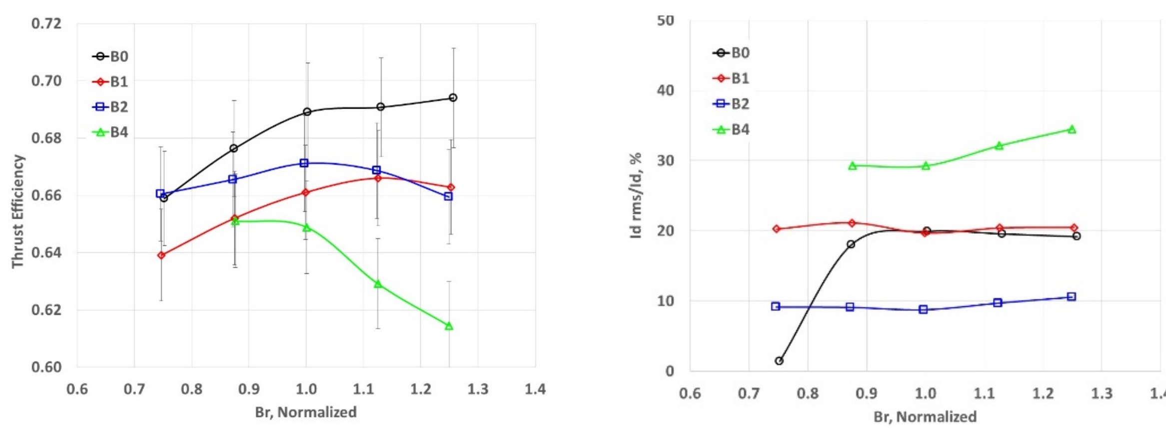

Figure 15. Magnetic Field Optimization performance and stability results for TDU-1 operating at 600 V, 12.5 kW [48]. Left: Thrust efficiency for B0, B1, B2, and B4 configurations. Right: Normalized discharge current RMS for B0, B1, B2, and B4 configurations.

D. TDU-2 environmental test campaign

Environmental testing of the HERMeS TDU-2 was conducted at JPL for the expected launch and deep-space environments [28]. The objectives of the environmental test campaign were to subject TDU-2 to random vibration and thermal cycling environments in order to:

1. Evaluate the thruster design and look for possible inherent issues with the design, and, in particular, demonstrate that the monolithic, large-diameter, BN-SiO_2 ceramic discharge chamber can survive qualification environments
2. Path find the execution of environmental tests for the AEPS engineering and qualification model thrusters, and
3. Gather data to validate and/or improve structural and thermal models.

To accomplish these objectives, TDU-2 was subjected to qualification level dynamic and thermal environments with periodic external physical inspections, magnetic field mappings and functional tests to verify operation or identify anomalies. The test flow from the environmental campaign is depicted in Figure 16. Figure 17 shows TDU-2 during the 3-axis random vibration and thermal cycling testing.

The HERMeS TDU-2 thruster successfully completed random vibrational and thermal vacuum qualification-level testing in 2018. Three-axis random vibration testing was performed in 2017 using a response limited excitation input to account for the shock isolation dampers incorporated in the AEPS thruster. Earlier random vibration testing in 2016 had revealed two design issues: fragmentation of the magnet coil potting material and structural weaknesses in the thruster-to-magnet coil bobbins. These issues were addressed with an alternate potting material selection and bobbin design revisions, enabling a successful retest of the thruster that demonstrated survivability of the ceramic discharge chamber with a load schedule of 10 g_{rms} over 120 seconds in each axis.

Thermal-vacuum testing in 2018 consisted of three temperature cycles from -121°C to +373°C with the thruster operating at 600 V, 12.5 kW including eight hours at peak temperature and a hot restart. A thermal model of the test configuration was developed and validated with the experimental results; an average difference of 5°C (1.7%) was observed between the model and the experiment.

Before and after the dynamic and thermal segments of this campaign, the thruster performance, plasma plume properties, thrust vector angle, discharge characteristics, and magnetic field topology were measured. Within measurement uncertainty, most of these parameters remained invariant the environmental test campaign. During the thermal testing, an increase in the discharge oscillation amplitude of 11% was observed as well as subtle thrust vector changes of $\pm 0.2°$ as the thruster warmed from -121°C to +373°C.

The HERMeS TDU-2 environmental testing campaign has paved the path for the AEPS ETU-1 thruster. ETU-1 recently passed acceptance level 3-axis Random Vibration testing at AR and was hot fired for the first time at JPL in August 2019 [10] (see Section IV below). Qualification-level random vibration, shock, and thermal cycling testing will be executed in the next few months. Overall, the TDU-2 environmental testing campaign, which represents the largest and highest-power Hall thruster ever to undergo vibration and thermal environmental qualification testing, has demonstrated the capability of surviving the launch and deep space environments needed to support future NASA missions.

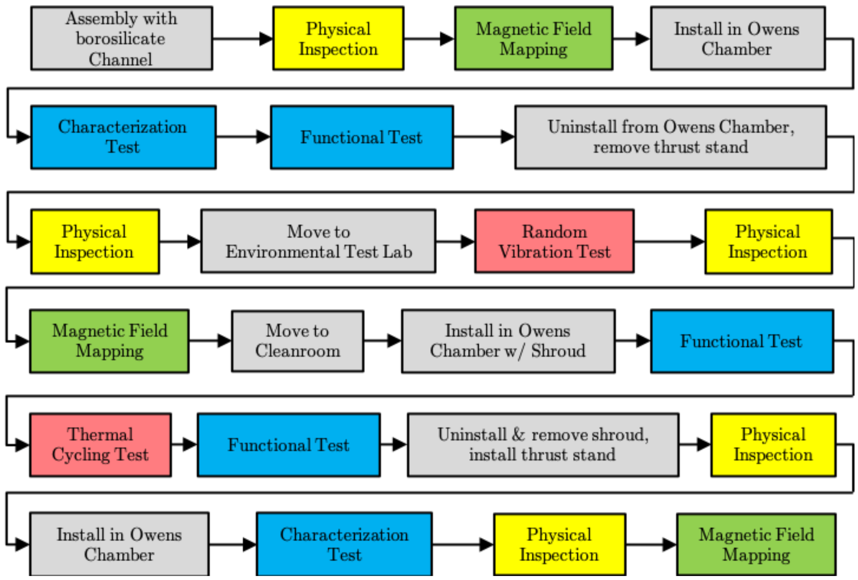

Figure 16 Test flow for the TDU-2 Environmental Test Campaign at JPL.

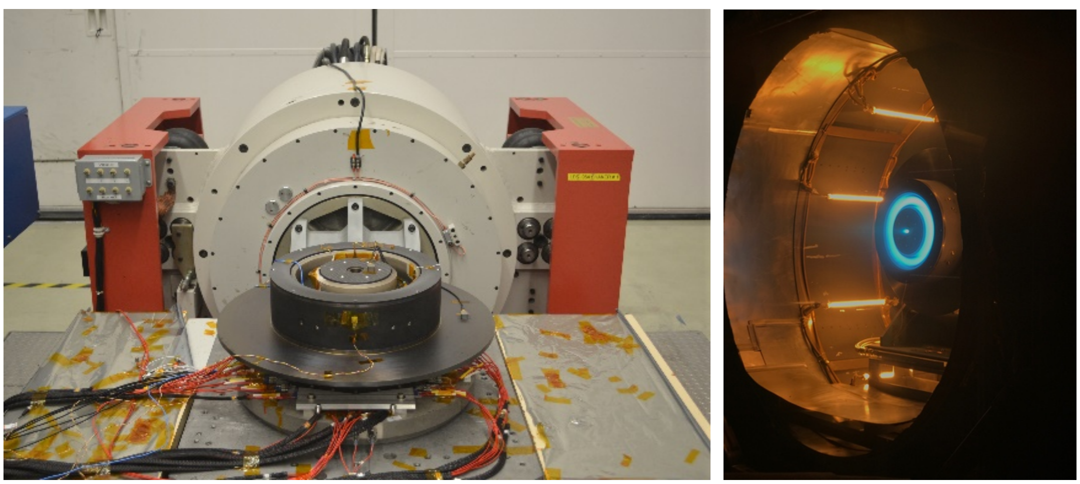

Figure 17 Environmental testing of HERMeS is used to demonstrate survivability from launch and deep-space conditions [28]. Left: HERMeS TDU-2 installed in the Environmental Test Laboratory at JPL prior to 3-axis random vibration testing. Right: TDU-2 firing at 12.5 kW, 600 V during thermal cycling testing in the Owens Chamber at JPL.

IV. AEPS Thruster Testing Status

Multiple vacuum facilities at GRC and JPL are being used to support AEPS thruster testing. In advance of this critical testing, pathfinder testing, such as the TDU-3 wear test or the TDU-2 environmental test, have been conducted to demonstrate the readiness of the chambers, diagnostics, and procedures. GRC's VF-5, which provides the highest pumping speed available in the nation for xenon electric thruster testing, will be used for performance testing, LIF testing, qualification wear testing, and hot-fire acceptance testing of the flight thrusters. JPL's Owens Chamber will be used to support qualification thermal cycle testing. Several components of the thruster, including the coil and cathode heaters, will also undergo qualification thermal cycle testing in JPL's Component Test Facility. Vacuum chambers at both GRC and JPL will be used to support cycle and wear testing of the AEPS cathode. Finally, electromagnetic interference (EMI) testing at a new facility at the Aerospace Corporation is planned.

AR has built upon the HERMeS thruster development investments to produce a thruster design with improved structural capability to survive the rigors of flight, a modified thermal management approach, and improvements to manufacturability, including incorporation of a flight-qualified electromagnetic coil fabrication process [9,10]. Two Engineering Test Units (ETU) have been fabricated by AR that proceed the qualification and flight builds. ETU-1 has completed assembly, acceptance-level 3-axis random vibration testing, and is currently in hot fire testing at JPL. Figure 18 shows ETU-1 integrated in the Owens Chamber at JPL and firing at the full-power condition of 600 V, 12.5 kW after achieving thermal steady-state operation at the nominal magnetic field intensity. Owing to the retention of key geometric and magnetic properties from HERMeS, initial results from measurements of performance, plasma oscillations, and plume properties on ETU-1 are consistent with the HERMeS thrusters. After hot fire testing, ETU-1 will undergo qualification-level random vibration testing at AR, shock testing at a commercial testing facility, and thermal cyclic testing at JPL followed by radiated emissions characterization testing planned for a new facility at The Aerospace Corporation. ETU-2 is in the final stages of assembly and will undergo hot fire performance, plasma characterization (including LIF measurements), and wear testing at GRC. As the testing of ETU-1 and assembly of ETU-2 are in progress at the time of this writing, further details will be available in future publications.

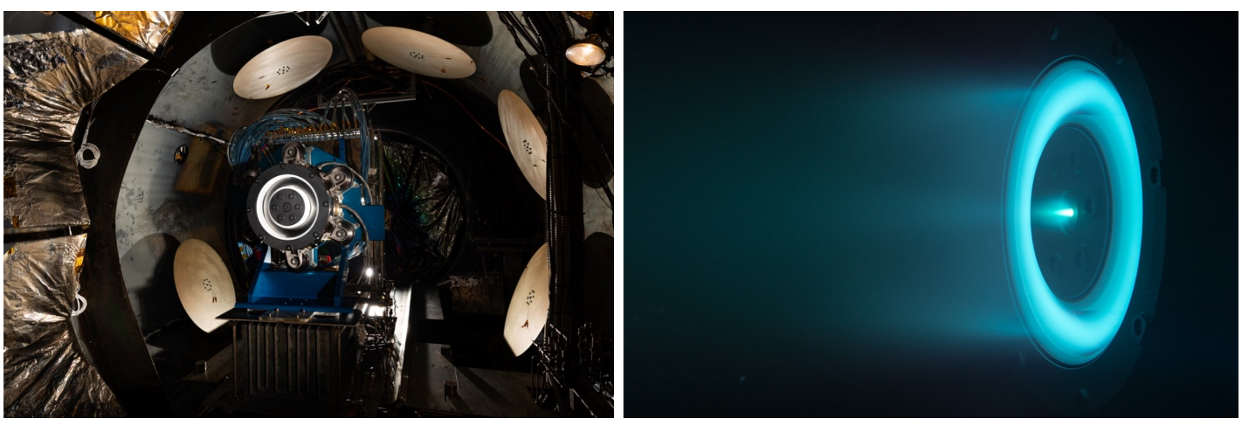

Figure 18. Left: The AEPS ETU-1 thruster installed in the Owens Chamber at JPL prior to first operation. Right: ETU-1 operation at 600 V, 12.5 kW after achieving thermal steady-state operation at the nominal magnetic field intensity.

V. Conclusion

With the development of HERMeS now complete, NASA uses the thruster hardware to conduct risk reduction and life qualification tasks supporting the AEPS thruster development. These have recently included various wear tests, plasma characterization and modeling for life qualification, magnetic field optimization, and environmental testing. First results from AEPS ETU-1 thruster testing show operation consistent with HERMeS and steady-state operation has been achieved at 600 V, 12.5 kW. The knowledge and experience gained through these tasks and others positions the program to advance to Critical Design Review with well understood risks and a credible plan to execute the life qualification of the AEPS thruster.

Acknowledgments

HERMeS is the result of a ridiculously talented team of professionals at GRC, JPL, Ohio Aerospace Institute, and Vantage Partners. We are extremely grateful for the contributions of these individuals and the organizations that support them. The support of the joint NASA GRC and JPL development of HERMeS by NASA's Space Technology Mission Directorate through the Solar Electric Propulsion Technology Demonstration Mission project is gratefully acknowledged. Portions of the research described in this paper were carried out at the Jet Propulsion Laboratory, California Institute of Technology, under a contract with the National Aeronautics and Space Administration.

References

[1] Trump, D. (Published in the Federal Register December 14, 2017, v.82 no.239, p.59501-59502). "Space Policy Directive 1: Reinvigorating America's Human Space Exploration Program " Retrieved August 21, 2019, from https://www.hsdl.org/?abstract&did=806399.

[2] Ticker, R., Gates, M., Manzella, D., Biaggi-Labiosa, A., and Lee, T., "The Gateway Power and Propulsion Element: Setting the Foundation for Exploration and Commerce," AIAA-2019-3811, August 2019.

[3] Strange, N., Landau, D., Polk, J., Brophy, J., and Mueller, J., "Solar Electric Propulsion for a Flexible Path of Human Space Exploration," Presented at the 61st International Astronautical Congress, IAC-10.A5.2.4, Prague, Czech Republic, Sep.-Oct., 2010.

[4] Brophy, J., Gershman, R., Strange, N., Landau, D. F., Merrill, R., and Kerslake, T., "300-kW Solar Electric Propulsion System Configuration for Human Exploration of near-Earth Asteroids," AIAA Paper 2011-5514, 2011.

[5] Mcguire, M. L., Hack, K. J., Manzella, D. H., and Herman, D. A., "Concept Designs for NASA's Solar Electric Propulsion Technology Demonstration Mission," AIAA Paper 2014-3717, July 2014.

[6] Manzella, D. and Hack, K., "High-Power Solar Electric Propulsion for Future NASA Missions," AIAA Paper 2014-3718, July 2014.

[7] Peterson, P. Y., "Overview of Nasa's Solar Electric Propulsion Project," Presented at the 36th International Electric Propulsion Conference, IEPC-2019-836, University of Vienna, Austria, September 15-20, 2019.

[8] Herman, D. A., "The Application of an Advanced Electric Propulsion System on the NASA Power and Propulsion Element (Ppe)," Presented at the 36th International Electric Propulsion Conference, IEPC-2019-651, University of Vienna, Austria, September 15-20, 2019.

[9] Jackson, J., Allen, M., Myers, R. M., Soendker, E., Welander, B., Tolentino, A., Hablitzel, S., Yeatts, C., Xu, S., Sheehan, C., Cardin, J., Snyder, J. S., Hofer, R. R., Tofil, T. et al., "13 kW Advanced Electric Propulsion Flight System Development and Qualification," Presented at the 35th International Electric Propulsion Conference, IEPC-2017-223, Atlanta, GA, Oct. 8 - 12, 2017, 2017.

[10] Jackson, J., Miller, S., Cassady, L., Myers, R., Soendker, E., Welander, B., Barber, M., and Peterson, P., "13kw Advanced Electric Propulsion Flight System Development and Qualification," Presented at the 36th International Electric Propulsion Conference, IEPC-2019-692, University of Vienna, Austria, September 15-20, 2019.

[11] Hofer, R., Polk, J., Mikellides, I., Lopez Ortega, A., Conversano, R., Chaplin, V., Lobbia, R., Goebel, D., Kamhawi, H., Verhey, T., Williams, G., Mackey, J., Huang, W., Yim, J. et al., "Development Status of the 12.5 kW Hall Effect Rocket with Magnetic Shielding (HERMeS)," Presented at the 35th International Electric Propulsion Conference, IEPC-2017-231, Atlanta, GA, Oct. 8 - 12, 2017, 2017.

[12] Becatti, G., Goebel, D. M., Polk, J. E., and Guerrero, P., "Life Evaluation of a Lanthanum Hexaboride Hollow Cathode for High-Power Hall Thruster," Journal of Propulsion and Power 34, 4, 893-900 (2018).

[13] Benavides, G. F., Mackey, J., Ahern, D., and Thomas, R., "Diagnostic for Verifying the Thrust Vector Requirement of the AEPS Hall-Effect Thruster and Comparison to the Next-C Thrust Vector Diagnostic," AIAA-2018-4514, July 2018.

[14] Chaplin, V. H., Jorns, B. A., Lopez Ortega, A., Mikellides, I. G., Conversano, R. W., Lobbia, R. B., and Hofer, R. R., "Laser-Induced Fluorescence Measurements of Acceleration Zone Scaling in the 12.5 kW HERMeS Hall Thruster," Journal of Applied Physics 124, 18 (2018).

[15] Choi, M. and Yim, J., "Development Status of a 3-D Electron Fluid Model for Hall Thruster Plume Simulations," AIAA-2018-4808, July 2018.

[16] De Groh, H. C., Geng, S. M., Niedra, J. M., and Hofer, R. R., "Magnetic Properties of Fe-49co-2v Alloy and Pure Fe at Room and Elevated Temperatures," NASA Technical Memorandum, NASA/TM-2018-219872, April 2018.

[17] Frieman, J. D., Ahern, D., Williams, G., Mackey, J., Haag, T., Huang, W., Kamhawi, H., Herman, D. A., Peterson, P. Y., Gilland, J. H., and Hofer, R. R., "In-Situ Diagnostic for Assessing Hall Thruster Wear," AIAA-2018-4721, July 2018.

[18] Frieman, J. D., Peterson, P. Y., Gilland, J. H., Kamhawi, H., Williams, G., Herman, D. A., and Hofer, R. R., "Long Duration Wear Test of the NASA HERMeS Hall Thruster," AIAA-2018-4645, July 2018.

[19] Frieman, J. D., Williams, G., Kamhawi, H., Sarver-Verhey, T., Herman, D., Peterson, P., Gilland, J., and Hofer, R., "Impact of Cathode and Keeper Configuration on HERMeS Thruster Operation," Presented at the 65th JANNAF Propulsion Meeting, Long Beach, CA, May 21-24, 2018.

[20] Guerrero, P., Polk, J. E., Lobbia, R. B., and Mikellides, I. G., "Determination of the Work Function Distribution of a LaB6 Hollow Cathode Based on Plasma Potential Measurement and 2d Plasma Numerical Simulation," AIAA-2018-4511, 2018.

[21] Hall, S. J., Sarver-Verhey, T. R., Frieman, J. D., Kamhawi, H., and Myers, J. L., "Preparation for Hollow Cathode Testing for the Advanced Electric Propulsion System at NASA Glenn Research Center," AIAA-2018-4425, July 2018.

[22] Huang, W., Kamhawi, H., and Herman, D., "A Laser-Induced Fluorescence Diagnostic for HERMeS and High-Power Electric Propulsion," Presented at the 65th JANNAF Propulsion Meeting, Long Beach, CA, May 21-24, 2018.

[23] Huang, W., Kamhawi, H., and Herman, D. A., "Ion Velocity in the Discharge Channel and Near-Field of the HERMeS Hall Thruster," AIAA-2018-4723, July 2018.

[24] Kamhawi, H., Huang, W., Gilland, J., Haag, T., Mackey, J., Yim, J., Pinero, L., Williams, G., Peterson, P., and Herman, D., "Performance, Stability, and Plume Characterization of the HERMeS Thruster with Boron Nitride Silica Composite Discharge Channel," Presented at the 65th JANNAF Propulsion Meeting, Long Beach, CA, May 21-24, 2018.

[25] Kamhawi, H., Huang, W., and Mikellides, I. G., "Optimization of the Magnetic Field Topology in the Hall Effect Rocket with Magnetic Shielding," AIAA-2018-4720, July 2018.

[26] Kamhawi, H., Mikellides, I., and Huang, W., "Optimization of the Magnetic Field Topology in the Hall Effect Rocket with Magnetic Shielding," Presented at the 65th JANNAF Propulsion Meeting, Long Beach, CA, May 21-24, 2018.

[27] Katz, I., Chaplin, V. H., and Lopez Ortega, A., "Particle-in-Cell Simulations of Hall Thruster Acceleration and near Plume Regions," Physics of Plasmas 25, 12 (2018).

[28] Lobbia, R. B., Conversano, R. W., Reilly, S., Hofer, R. R., and Sorensen, R., "Environmental Testing of the HERMeS TDU-2 Hall Thruster," AIAA-2018-4646, July 2018.

[29] Lopez Ortega, A., Katz, I., and Chaplin, V. H., "Application of a First-Principles Anomalous Transport Model for Electrons to Multiple Hall Thrusters and Operating Conditions," AIAA-2018-4903, July 2018.

[30] Lopez Ortega, A. and Mikellides, I. G., "Investigations of Pole Erosion Mechanisms in the 12.5 kW HERMeS Hall Thruster with the Hall2De Code," AIAA-2018-4647, July 2018.

[31] Mackey, J., Hall, S. J., Haag, T., Peterson, P. Y., and Kamhawi, H., "Uncertainty in Inverted Pendulum Thrust Measurements," AIAA-2018-4516, July 2018.

[32] Mackey, J., Salem, J., Kamhawi, H., McEnerney, B., Hofer, R., Johnson, M., Faber, K., and Peterson, P., "Evaluation of Boron Nitride Materials for Hall Thruster Discharge Channels," Presented at the 65th JANNAF Propulsion Meeting, Long Beach, CA, May 21-24, 2018.

[33] Mikellides, I. G., Guerrero, P., Lopez Ortega, A., and Polk, J. E., "Spot-to-Plume Mode Transition Investigations in the HERMeS Hollow Cathode Discharge Using Coupled 2-D Axisymmetric Plasma-Thermal Simulations," AIAA-2018-4722, July 2018.

[34] Peterson, P. Y., Frieman, J., Kamhawi, H., Williams, G., Herman, D., Gilland, J., and Hofer, R., "NASA HERMeS Hall Thruster Long Duration Wear Test," Presented at the 65th JANNAF Propulsion Meeting, Long Beach, CA, May 21-24, 2018.

[35] Polk, J. E. and Brophy, J. R., "Life Qualification of Hall Thrusters by Analysis and Test," Presented at the Space Propulsion 2018 Conference, Paper No. 547, Seville, Spain, May 14-18, 2018.

[36] Lopez Ortega, A., Mikellides, I. G., Sekerak, M. J., and Jorns, B. A., "Plasma Simulations in 2-D (R-Z) Geometry for the Assessment of Pole Erosion in a Magnetically Shielded Hall Thruster," Journal of Applied Physics 125, 3 (2019).

[37] Huang, W. and Yim, J., "Propellant Distributor for a Thruster," United States Patent No. 10,273,944 (April 30, 2019).

[38] Chaplin, V. H., Lobbia, R. B., Lopez Ortega, A., Mikellides, I. G., Roberts, P. J., Peter, J. S., Hofer, R. R., Polk, J. E., and Friss, A. J., "Spatiotemporally Resolved Ion Velocity Distribution Measurements in the 12.5 kW HERMeS Hall Thruster," Presented at the 36th International Electric Propulsion Conference, IEPC-2019-532, University of Vienna, Austria, September 15-20, 2019.

[39] Frieman, J., "Impact of Facility Pressure on the Wear of the NASA HERMeS Hall Thruster," Presented at the 36th International Electric Propulsion Conference, IEPC-2019-714, University of Vienna, Austria, September 15-20, 2019.

[40] Gray, T., "Non-Intrusive Characterization of the Wear of the HERMeS Thruster Using Optical Emission Spectroscopy " Presented at the 36th International Electric Propulsion Conference, IEPC-2019-841, University of Vienna, Austria, September 15-20, 2019.

[41] Huang, W., "Variation in Ion Acceleration Characteristics of the HERMeS Hall Thruster During Magnetic Optimization," Presented at the 36th International Electric Propulsion Conference, IEPC-2019-713, University of Vienna, Austria, September 15-20, 2019.

[42] Huang, W., Kamhawi, H., and Herman, D. A., "Evidence of Counter-Streaming Ions near the Inner Pole of the HERMeS Hall Thruster," AIAA-2019-3897, August 2019.
[43] Mackey, J., Frieman, J., Ahern, D., and Gilland, J., "Uncertainty in Electric Propulsion Erosion Measurements," AIAA-2019-3896, August 2019.
[44] Lobbia, R. B., Polk, J. E., Hofer, R. R., Chaplin, V. H., and Jorns, B. A., "Accelerating 23,000 Hours of Ground Test Backsputtered Carbon on a Magnetically Shielded Hall Thruster," AIAA-2019-3898, August 2019.
[45] Frieman, J. D., Kamhawi, H., Mackey, J., Haag, T., Peterson, P. Y., Herman, D. A., Gilland, J., and Hofer, R. R., "Completion of the Long Duration Wear Test of the NASA HERMeS Hall Thruster," AIAA-2019-3895, August 2019.
[46] Hall, S., "The Role of Neutral Pressure Due to Anode Geometry in Hollow Cathode Mode Transitions," Presented at the 36th International Electric Propulsion Conference, IEPC-2019-300, University of Vienna, Austria, September 15-20, 2019.
[47] Baird, M., "Development and Validation of a Time-Resolved Ion Energy Distribution Diagnostic," Presented at the 36th International Electric Propulsion Conference, IEPC-2019-515, University of Vienna, Austria, September 15-20, 2019.
[48] Kamhawi, H., "Performance, Plume, Stability, and Wear Characterization of Three Alternate Magnetic Field Topologies in the Hall Effect Rocket with Magnetic Shielding," Presented at the 36th International Electric Propulsion Conference, IEPC-2019-902, University of Vienna, Austria, September 15-20, 2019.
[49] Hofer, R., Kamhawi, H., Herman, D., Polk, J., Snyder, J. S., Mikellides, I., Huang, W., Myers, J., Yim, J., Williams, G., Lopez Ortega, A., Jorns, B., Sekerak, M., Griffiths, C. et al., "Development Approach and Status of the 12.5 kW HERMeS Hall Thruster for the Solar Electric Propulsion Technology Demonstration Mission," Presented at the 34th International Electric Propulsion Conference, IEPC-2015-186, Kobe, Japan, July 4-10, 2015.
[50] Hofer, R. R., Kamhawi, H., Mikellides, I., Herman, D., Polk, J., Huang, W., Yim, J., Myers, J., and Shastry, R., "Design Methodology and Scaling of the 12.5 kW HERMeS Hall Thruster for the Solar Electric Propulsion Technology Demonstration Mission," Presented at the 62nd JANNAF Propulsion Meeting, JANNAF-2015-3946, Nashville, TN, June 1-5, 2015.
[51] De Grys, K. H., Mathers, A., Welander, B., and Khayms, V., "Demonstration of 10,400 Hours of Operation on 4.5 kW Qualification Model Hall Thruster," AIAA Paper 2010-6698, July 2010.
[52] Mikellides, I. G., Katz, I., Hofer, R. R., Goebel, D. M., De Grys, K. H., and Mathers, A., "Magnetic Shielding of the Acceleration Channel in a Long-Life Hall Thruster," Physics of Plasmas 18, 033501 (2011).
[53] Mikellides, I. G., Katz, I., Hofer, R. R., and Goebel, D. M., "Magnetic Shielding of Walls from the Unmagnetized Ion Beam in a Hall Thruster," Applied Physics Letters 102, 2, 023509 (2013).
[54] Hofer, R. R., Goebel, D. M., Mikellides, I. G., and Katz, I., "Magnetic Shielding of a Laboratory Hall Thruster Part II: Experiments," Journal of Applied Physics 115, 043303 (2014).
[55] Mikellides, I. G., Katz, I., Hofer, R. R., and Goebel, D. M., "Magnetic Shielding of a Laboratory Hall Thruster Part I: Theory and Validation," Journal of Applied Physics 115, 043303 (2014).
[56] Hofer, R. R., Goebel, D. M., Mikellides, I. G., and Katz, I., "Design of a Laboratory Hall Thruster with Magnetically Shielded Channel Walls, Phase II: Experiments," AIAA-2012-3788, July 2012.
[57] Hofer, R. R., Jorns, B. A., Polk, J. E., Mikellides, I. G., and Snyder, J. S., "Wear Test of a Magnetically Shielded Hall Thruster at 3000 Seconds Specific Impulse," Presented at the 33rd International Electric Propulsion Conference, IEPC-2013-033, Washington, DC, Oct 6-10, 2013.
[58] Mikellides, I. G., Hofer, R. R., Katz, I., and Goebel, D. M., "Magnetic Shielding of Hall Thrusters at High Discharge Voltages," Journal of Applied Physics 116, 5, 053302 (2014).
[59] Kamhawi, H., Huang, W., Haag, T., Shastry, R., Soulas, G., Smith, T., Mikellides, I. G., and Hofer, R. R., "Performance and Thermal Characterization of the NASA-300ms 20 kW Hall Effect Thruster," Presented at the 33rd International Electric Propulsion Conference, IEPC-2013-444, Washington, DC, Oct 6-10, 2013.
[60] Piragino, A., Giannetti, V., Reza, M., Faraji, F., Ferrato, E., Kitaeva, A., Pedrini, D., Andreussi, T., Andrenucci, M., and Paganucci, F., "Development Status of Sitael's 20 kW Class Hall Thruster," AIAA-2019-3812, August 2019.
[61] Conversano, R. W., Goebel, D. M., Hofer, R. R., Mikellides, I. G., and Wirz, R. E., "Performance Analysis of a Low-Power Magnetically Shielded Hall Thruster: Experiments," Journal of Propulsion and Power 33, 4, 975-983 (2017).
[62] Grimaud, L. and Mazouffre, S., "Ion Behavior in Low-Power Magnetically Shielded and Unshielded Hall Thrusters," Plasma Sources Science and Technology 26, 5 (2017).
[63] Hofer, R. R., Jorns, B. A., Brophy, J. R., and Katz, I., "Hall Effect Thruster Electrical Configuration," California Institute of Technology, USPTO patent application submitted, March 30 2017.
[64] Snyder, J. S., Goebel, D. M., Chaplin, V., Lopez Ortega, A., Mikellides, I. G., Aghazadeh, F., Johnson, I., Kerl, T., and Lenguito, G., "Electric Propulsion for the Psyche Mission," Presented at the 36th International Electric Propulsion Conference, IEPC-2019-244, Vienna, Austria, Sept. 15-20, 2019.
[65] Jorns, B. A., Dodson, C., Anderson, J., Goebel, D. M., Hofer, R. R., Sekerak, M., Lopez Ortega, A., and Mikellides, I., "Mechanisms for Pole Piece Erosion in a 6-kW Magnetically-Shielded Hall Thruster," AIAA-2016-4839, July 2016.
[66] Williams, G. J., Gilland, J. H., Peterson, P. Y., Kamhawi, H., Huang, W., Ahern, D. W., Yim, J., Herman, D. A., Hofer, R. R., and Sekerak, M., "Wear Testing of the HERMeS Thruster," AIAA-2016-5025, July 2016.
[67] Sekerak, M. J., Hofer, R. R., Polk, J. E., Jorns, B. A., and Mikellides, I. G., "Wear Testing of a Magnetically Shielded Hall Thruster at 2000 S Specific Impulse," Presented at the 34th International Electric Propulsion Conference, IEPC-2015-155, Kobe, Japan, July 4-10, 2015.

[68] Goebel, D. M., Jorns, B., Hofer, R. R., Mikellides, I. G., and Katz, I., "Pole-Piece Interactions with the Plasma in a Magnetically Shielded Hall Thruster," AIAA Paper 2014-3899, July 2014.
[69] Polk, J. E., Lobbia, R. B., Barriault, A., Guerrero, P., Mikellides, I., and Lopez Ortega, A., "Inner Front Pole Erosion in the 12.5 kW HERMeS Hall Thruster over a Range of Operating Conditions," Presented at the 35th International Electric Propulsion Conference, IEPC-2017-409, Atlanta, GA, Oct. 8 - 12, 2017, 2017.
[70] Williams, G., Kamhawi, H., Choi, M., Haag, T. W., Huang, W., Herman, D., Gilland, J. H., and Peterson, P. Y., "Wear Trends of the HERMeS Thruster as a Function of Throttle Point," Presented at the 35th International Electric Propulsion Conference, IEPC-2017-207, Atlanta, GA, Oct. 8 - 12, 2017, 2017.
[71] Sengupta, A., Anderson, J. A., Garner, C., Brophy, J. R., De Groh, K. K., Banks, B. A., and Karniotis Thomas, T. A., "Deep Space 1 Flight Spare Ion Thruster 30,000-Hour Life Test," Journal of Propulsion and Power 25, 1, 105-117 (2009).
[72] Polk, J. E., Anderson, J. R., Brophy, J. R., Rawlin, V. K., Patterson, M. J., Sovey, J., and Hamley, J., "An Overview of the Results from an 8200 Hour Wear Test of the Nstar Ion Thruster," AIAA Paper 1999-2446, June 1999.
[73] Gilland, J., Williams, G. J., Burt, J. M., and Yim, J. T., "Carbon Back Sputter Modeling for Hall Thruster Testing," AIAA-2016-4941, July 2016.
[74] Williams, G. J., Gilland, J. H., Peterson, P. Y., Kamhawi, H., Huang, W., Ahern, D. W., Yim, J., Herman, D. A., and Hofer, R. R., "Wear-Testing of the 12.5 kW HERMeS Technology Demonstration Unit One," Presented at the 63rd JANNAF Propulsion Meeting, Dec. 5-8, 2016.
[75] Hofer, R. R., Cusson, S. E., Lobbia, R. B., and Gallimore, A. D., "The H9 Magnetically Shielded Hall Thruster," Presented at the 35th International Electric Propulsion Conference, IEPC-2017-232, Atlanta, GA, Oct. 8-12, 2017, 2017.
[76] Goebel, D. M., Hofer, R. R., Mikellides, I. G., Katz, I., Polk, J. E., and Dotson, B. N., "Conducting Wall Hall Thrusters," IEEE Transactions on Plasma Science 43, 1, 118-126 (2015).
[77] Mikellides, I. G. and Katz, I., "Numerical Simulations of Hall-Effect Plasma Accelerators on a Magnetic-Field-Aligned Mesh," Physical Review E 86, 4, 046703 (2012).
[78] Ortega, A. L. and Mikellides, I. G., "The Importance of the Cathode Plume and Its Interactions with the Ion Beam in Numerical Simulations of Hall Thrusters," Physics of Plasmas 23, 4, 043515 (2016).
[79] Katz, I. and Mikellides, I. G., "Neutral Gas Free Molecular Flow Algorithm Including Ionization and Walls for Use in Plasma Simulations," J. Comput. Phys. 230, 4, 1454-1464 (2011).
[80] Lopez Ortega, A., Mikellides, I. G., and Jorns, B. A., "First-Principles Modeling of the Iat-Driven Anomalous Resistivity in Hollow Cathode Discharges II: Numerical Simulations and Comparison with Experiments," AIAA-2016-4627, July 2016.
[81] Mikellides, I. G. and Katz, I., "Wear Mechanisms in Electron Sources for Ion Propulsion, 1: Neutralizer Hollow Cathode," Journal of Propulsion and Power 24, 4, 855 (2008).
[82] Mikellides, I. G., Katz, I., Goebel, D. M., Jameson, K. K., and Polk, J. E., "Wear Mechanisms in Electron Sources for Ion Propulsion, 2: Discharge Hollow Cathode," Journal of Propulsion and Power 24, 4, 866 (2008).
[83] Mikellides, I. G., Katz, I., Goebel, D. M., and Polk, J. E., "Hollow Cathode Theory and Experiment. II. A Two-Dimensional Theoretical Model of the Emitter Region," Journal of Applied Physics 98, 113303 (2005).
[84] Yim, J. T. and Burt, J. M., "Characterization of Vacuum Facility Background Gas through Simulation and Considerations for Electric Propulsion Ground Testing," AIAA-2015-3825, July 2015.
[85] Yim, J., "A Survey of Xenon Ion Sputter Yield Data and Fits Relevant to Electric Propulsion Spacecraft Integration," Presented at the 35th International Electric Propulsion Conference, IEPC-2017-060, Atlanta, GA, Oct. 8 - 12, 2017, 2017.
[86] Lopez Ortega, A., Mikellides, I., and Goebel, D. M., "Numerical Simulations for Life Assessments of the BaO and LaB6 Cathode Options in the Hall Effect Rocket with Magnetic Shielding (HERMeS)," Presented at the 35th International Electric Propulsion Conference, IEPC-2017-152, Atlanta, GA, Oct. 8 - 12, 2017, 2017.
[87] Chaplin, V. H., Conversano, R. W., Lobbia, R. B., Lopez Ortega, A., Mikellides, I. G., Hofer, R. R., and Jorns, B. A., "Laser Induced Fluorescence Measurements of the Acceleration Zone in the 12.5 kW HERMeS Hall Thruster," Presented at the 35th International Electric Propulsion Conference, IEPC-2017-229, Atlanta, GA, Oct. 8 - 12, 2017, 2017.
[88] Lopez Ortega, A., Mikellides, I., and Chaplin, V., "Numerical Simulations for the Assessment of Erosion in the 12.5-kW Hall Effect Rocket with Magnetic Shielding (HERMeS)," Presented at the 35th International Electric Propulsion Conference, IEPC-2017-154, Atlanta, GA, Oct. 8 - 12, 2017, 2017.
[89] Lopez Ortega, A., Mikellides, I. G., Conversano, R., Lobbia, R. B., and Chaplin, V. H., "Plasma Simulations for the Assessment of Pole Erosion in the Magnetically Shielded Miniature Hall Thruster (Masmi)," Presented at the 36th International Electric Propulsion Conference, IEPC-2019-281, Vienna, Austria, Sept. 15-20, 2019.
[90] Durot, C. J., "Development of a Time-Resolved Laser-Induced Fluorescence Technique for Nonperiodic Oscillations," Ph.D. dissertation, Applied Physics, University of Michigan, Ann Arbor, MI, 2016.
[91] Lobbia, R. B. and Gallimore, A. D., "A Method of Measuring Transient Plume Properties," AIAA-2008-4650, July 2008.
[92] Shastry, R., Huang, W., and Kamhawi, H., "Near-Surface Plasma Characterization of the 12.5-kW NASA TDU1 Hall Thruster," AIAA-2015-3919, July 2015.